Towards Bendable CMOS Magnetic Sensors

Hadi Heidari*, Nicoleta Wacker, Scott Roy*, Ravinder Dahiya*†
*Electronics and Nanoscale Engineering Division, University of Glasgow, G12 8QQ, UK
†Correspondence to - Ravinder.Dahiya@glasgow.ac.uk

***Abstract*—This paper analyses the bending-induced stress effects on ultra-thin cross-shaped magnetic sensors operating in voltage- or current-modes. Both the magnetic sensor's sensitivity and the offset drift have been analysed. The optimum geometry and thickness of the Hall sensor are the important parameters to be analysed to compensate any mechanical stress related effect on the performance of sensors. Numerical simulations are carried out using the finite element method (FEM) with COMSOL Multiphysics® software. A compact model is implemented in Verilog-A and used for the simulations in Cadence© Spectre, considering a 350 nm CMOS process. The simulation results focus on magnetic sensor's sensitivity variation and offset drift induced by bending of the substrate. The simulation results show a sensitivity of 71 V/AT at 100 mT. Interestingly, the sensitivity variation induced by 250 MPa applied uniaxial stress is less than 0.02 %.**

***Index Terms*—Flexible Electronics, Piezo-Hall Effect, Piezoresistive Effect, Magnetic Sensor.**

I. Introduction

Electronic or tactile skin is currently being investigated to enable advances in a number of areas including safe interaction in robotics, advanced prosthetics, and biomedical electronics [1]–[3]. It involves integrating multiple functionalities such as sensors and electronic on flexible or bendable substrates [4]. Inspired from human sense of touch, the sensors that have often been investigated for electronic skin are meant to measure pressure and temperature [1], [2]. However it will be useful to go beyond imitating the human skin functionality and introduce new sensors such as magnetic sensors. The e-skin with magnetic sensor could be useful in numerous application areas including biomedical devices [5], wearable electronics [6] and robotics [7]. For example, the capability to perceive the presence of static or dynamic magnetic field will allow using electronic skin in tasks such as magnetic manipulation of an untethered object in an unrestricted workspace for applications ranging from wind-tunnel model stabilization, to medical device control, to microrobotic manipulation [8]. The magnetic sensors with on–chip signal processing capability, realized with complementary metal-oxide-semiconductor (CMOS) technologies will open interesting avenues for flexible electronics. This requires the magnetic sensors chip to be bendable or at least conformable. This underlines the need to investigate the effect of stress and bending on the performance of magnetic sensors.

The bending-induced strain alters the performance of CMOS magnetic sensors in terms of sensitivity and offset voltage [9], [10]. Their accurate functionality during bending requires minimization/compensation of the stress effects on their performance. The design challenges include selection of the optimum orientation of the sensor with respect to the crystal lattice of silicon (Si) and the use of a signal-processing circuit that compensates the effects of both in-plane bending-induced uniaxial stress and temperature. In this paper we analyze the magnetic sensor's behavior under different strain conditions by modeling and simulation. A model is built in Verilog-A© for simulations in Cadence© Spectre. Finite element method (FEM) simulations are performed with COMSOL Multiphysics® software, and the results compared.

The paper is organized as follows: Section II contains theoretical aspects of cross-shaped magnetic sensors. Simulation and modeling of an ultra-thin strained magnetic sensor are presented in Section III. This section includes FEM simulation in Section III-A and compact model in Verilog-A in Section III-B. The simulation results are compared and discussed in Section IV. Finally, the conclusions are given in Section V.

II. CMOS Hall Sensors

The cross-shaped CMOS Hall-effect sensor is widely used because of its high sensitivity and compatibility with the standard CMOS process. As shown in Figure 1, this 90^o-rotation invariant geometry consists of an N-well (e.g. $n = 1.8\times10^{15}$ cm^{-3} for a 350 nm CMOS process doped diffusion region ($H_{N-well} \sim 2$ μm thick) in an ultra-thin P-substrate ($H_{P-sub} \sim 20$ μm thick). A shallow heavily doped top P+ layer covers the surface of the active area, allowing a higher current-related sensitivity by reducing the conducting layer thickness [11], [12]. At each end of the cross there are four contact regions highly N+ doped to reduce the contact resistances in the source and drain formation processing step

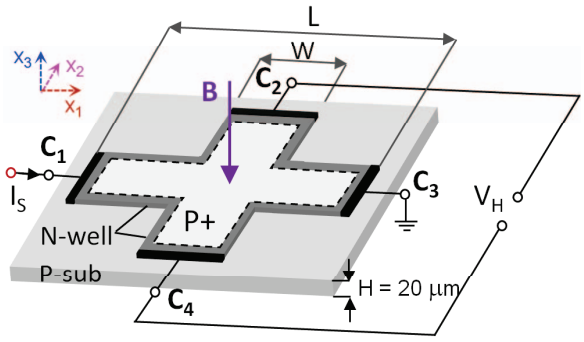

Fig. 1. Cross-shaped horizontal CMOS Hall-effect sensor. **B** is the applied magnetic field and (x_1, x_2) is the in-plane cartesian coordinate system.

for n-type MOSFETs. The lateral dimensions (L, W) are chosen so as to obtain high output accuracy ($W/2L \cong 1.31$) [13].

Subjected to both a magnetic field **B** orthogonally applied to its plane and a current I_S applied between two contacts (e.g. C_1−C_3), the carriers will be deviated by the Lorentz force [14] and a Hall voltage V_H appears between the other two contacts (C_2−C_4) [15]. The output voltage is directly proportional to the applied magnetic field [13]

$$V_H = G \cdot \frac{r_H}{qn \cdot h} \cdot I_S \cdot |\mathbf{B}| = S_I \cdot I_S \cdot |\mathbf{B}| \qquad (1)$$

where G is the geometrical correction factor, $r_H(Si) = 1.15$ the scattering factor, n and h the doping and thickness of the N-well and S_I the current-related sensitivity [13].

Deformations can induce considerable mechanical stress in CMOS Hall-effect sensors via the piezo-Hall effect, [16], and may change the magnetic sensitivity. Since a Hall sensor is both magnetic- and stress-sensitive, it can be used in both cases. However, in order to determine accurately the magnetic field strength when the sensor is deformed mechanically, the piezoresistive effect [17] must be compensated, [13], [18].

Mechanical stress changes the electrical resistance of Si by changing its resistivity [19], affecting the current-related sensitivity $S_I = \frac{V_H}{I_S \cdot |\mathbf{B}|}$ of the magnetic sensor (piezo-Hall effect) [16]. By considering the plane-stress assumption ($\sigma_{33} \cong 0$) [20] the sensitivity variation with stress can be expressed as:

$$S_I(\sigma, V, T) = S_I(V, T) \cdot [1 + P_{12} \cdot (|\boldsymbol{\sigma_{11}}| + |\boldsymbol{\sigma_{22}}|)] \qquad (2)$$

where P_{12} is the piezo-Hall coefficient in (x_1, x_2)-plane. P_{12}=40×10^{-11} Pa^{-1} for an N-well with n=4×10^{16} cm^{-3} [16]. $\boldsymbol{\sigma_{11}}$ and $\boldsymbol{\sigma_{22}}$ are the in-plane stress $\boldsymbol{\sigma}$ components along [100] and [010] axes (see Figure 5).

III. Hall Sensor Simulation and Modeling

Since the sensor to be integrated in Cadence environment with bias and readout circuits, a four-resistor Verilog-A compact model implemented based on physical and mechanical point of view in FEM simulation results. accordingly, in this section we present the numerical results obtained by 3D simulations in COMSOL Multiphysics® and compare them with those obtained in Cadence© Spectre. A thin cross-shaped magnetic sensor is modelled and strained uniaxially by using the four-point bending (4PB) test. The effects of uniaxial stress on sensor's sensitivity are analyzed.

A. FEM simulation

The ultra-thin magnetic sensor is deformed uniaxially using the four-point bending (4PB) flexural test [20]. Although this bending method is most frequently applied to investigate thick samples, it can be adapted for thin samples as well. The principle of the 4PB test is shown in Figure 2. Two equal lateral loads are applied transversely and simultaneously on two edges of the sample. The loads create two couples **M** about the X_2-axis, that deform the sample into a curved plane inducing a maximum tensile uniaxial stress $+|\boldsymbol{\sigma_{11}}|$ at the top and a maximum compressive stress $-|\boldsymbol{\sigma_{11}}|$ on the opposite surface of the sample. Stress decreases towards the neutral surface (in red) where is 0. The material is considered isotropic. According to Poisson's effect [20], a compressive stress $|\boldsymbol{\sigma_{22}}| = -\nu \cdot |\boldsymbol{\sigma_{11}}|$ is induced along the X_2-axis. The Poisson's ratio of Si $\nu_{<100>/(001)}$=0.279 [21].

Thin structures undergo large deformation and the assumption of small deflections is not valid anymore. In that case the bending-induced uniaxial stress can be calculated using the radius of curvature R as

$$\sigma_{11} = E \cdot \frac{x_3}{R} = E \cdot \frac{H}{2R} \qquad (3)$$

where E is the elasticity modulus of Si ($E_{<100>/(001)}$ = 130.2 GPa) and X_3 [21] is the distance from the neutral surface to the point of interest (e.g. $X_3 = H/2$). According to (3), a bending radius of $R = 10$ mm would result in a tensile uniaxial stress induced in sensor $|\boldsymbol{\sigma_{11}}| \cong 170$ MPa.

Finite element method (FEM) numerical simulation in COMSOL Multiphysics® is used to predict the sensor's performance in both flat and bent states. The model of a cross-shaped magnetic sensor was built, mesh sensitivity investigated and the sensor's electromechanical behaviour was simulated. We analyse the case $X_1 \parallel \boldsymbol{\sigma} \parallel [100]$. The uniaxial stress $|\boldsymbol{\sigma_{11}}|$ distribution induced by bending is shown in the example presented in Figure 3. Although in the central region of the sensor the uniaxial stress is uniform, larger stress values can be noticed in the region close to the edges, located along the X_2-axis, in accordance with [22].

The stress-induced sensors's sensitivity variation for different strengths of the magnetic fields ($|\mathbf{B}|$=$\{25, 50, 100\}$ mT) is further investigated. The structure in Figure 2 is biased by a current I_S=1 mA applied along [100] Si-direction and the Hall voltage V_H in the transversal direction [010] is recorded. The simulation results show that the current-related sensitivity in the flat state is $S_I \cong 71$ V/AT, which is in agreement with [18].

The surface electric potential and the current density vector field distributions in the flat and bent states in the presence of $|\mathbf{B}|$=100 mT are shown in Figure 4 (a) and (b) respectively. The results show that ($\sim 200-250$ MPa) stress has negligible

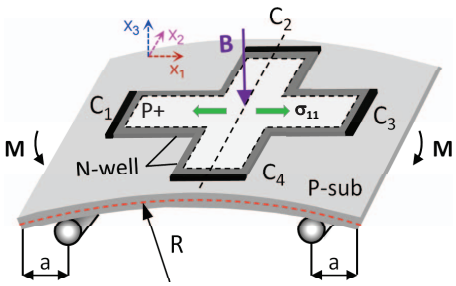

Fig. 2. Four-point bending (4PB) classical flexural test. $\boldsymbol{\sigma_{11}}$ is the induced tensile uniaxial stress and R is the bending radius. The neutral surface is shown in red. **M** are the applied couples.

effect on the field distribution. Moreover, the sensor's sensitivity variation induced by 250 MPa uniaxial stress at different applied magnetic fields, is less than 0.02 %.

B. Verilog-A Model

The magnetic sensor is modelled as a full conventional 4-resistance Wheatstone bridge, as shown in Figure 5. The Wheatstone bridge is also well suited for the measurement of strain-induced variations in resistances. Therefore, it is also suitable for measuring the resistance changes in a strain gage. The diagonal resistances are neglected. The in-plane cartesian coordinate system (X_1, X_2) attached to the bridge is chosen so that $X_1 \| [100]$ and $X_2 \| [010]$ (θ=0). The angle θ defines the position of the bridge with respect to $[100]$ and φ the uniaxial stress application direction.

The voltage-mode and the current-mode of operation define different boundary conditions. Hence, the magnetic field affect differently the current flow in the device. In order to obtain first approximation results we assume that same resistor variations in both modes of operation. Further on, the Verilog-A model is introduced and the results of simulations in Cadence© Spectre presented. The magnetic sensor model was implemented using Verilog-A© language so that it can be simulated and tested in Cadence© Spectre. In the absence of external magnetic field and mechanical stress, all four resistors have the same initial value R_0=1.5 kΩ, calculated as:

$$R_0 = \frac{1}{q \cdot \mu_n \cdot n \cdot H} \tag{4}$$

or determined in two steps: (i) the node C_3 is grounded and 1 mA are applied to the terminal C_1. (ii) The terminal C_1 is grounded and the current is applied to terminal C_3. In above equation, $q = 1.602\times10^{-19}$ C is electron charge and $\mu_n \cong 1150$ cm^2/Vs is the electrons mobility for the aforementioned doping n.

In order to account for resistance variation induced by both piezo-Hall and piezoresistive effects, the value of each resistor is expressed as a function of five parameters $(R_0, \beta, |\mathbf{B}|, |\boldsymbol{\sigma}|, \Pi)$

$$R = R_0(1 \pm \beta|\mathbf{B}| \pm \Pi|\boldsymbol{\sigma}|) \tag{5}$$

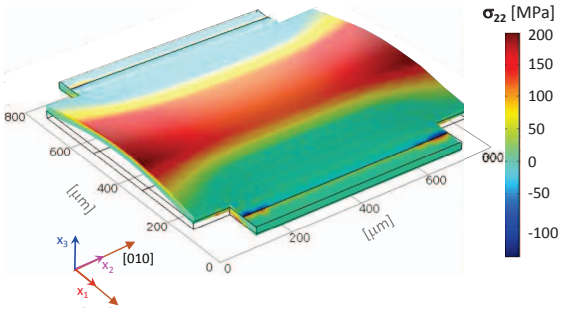

Fig. 3. Bending induced uniaxial stress distribution: COMSOL simulation of the σ_{11} distribution in the ultra-thin magnetic sensor induced by the 4PB test.

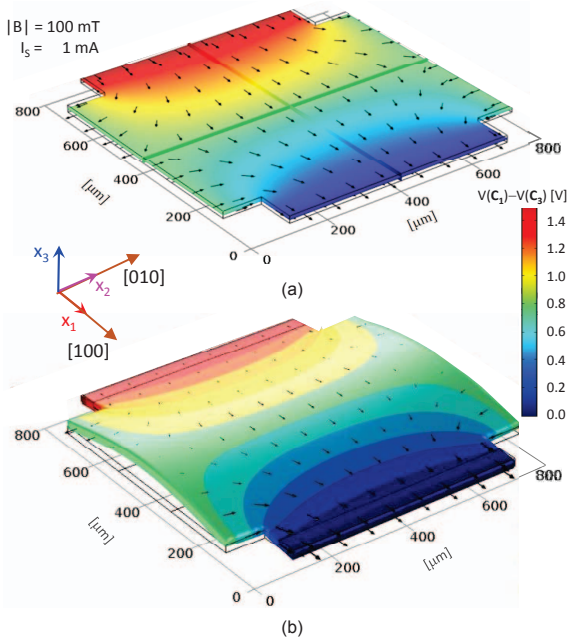

Fig. 4. Electric potential distribution and current density vector field: 3D COMSOL simulation of the cross-shaped Hall sensor showing the distribution of the electric potential and the current density vector field, for $|B| = 100$ mT and $I_S = 1$ mA applied along [010]: (a) flat-state; (b) bent-state corresponding to the bending-induced $|\boldsymbol{\sigma_{22}}| \cong 200$ MPa.

where β the magnetic resistance coefficient, defined as the average of initial values of resistors R_0 in the presence and absence of the magnetic field (**B**). Π is the general piezoresistive coefficient for (001) Si-plane [23]. It can be expressed as a function of the fundamental Si piezoresistive coefficients $(\Pi_{11}, \Pi_{12}, \Pi_{44})$ [17] and angles θ and φ

$$\begin{aligned}\Pi(\theta,\varphi) = \Pi_{11} \cdot (\cos^2\theta \cdot \cos^2\varphi + \sin^2\theta \cdot \sin^2\varphi) \\ + \Pi_{12} \cdot (\cos^2\theta \cdot \sin^2\varphi + \sin^2\theta \cdot \cos^2\varphi) \\ + 2 \cdot \Pi_{44} \cdot \sin\theta \cdot \cos\theta \cdot \sin\varphi \cdot \cos\varphi\end{aligned} \tag{6}$$

For resistors oriented $\theta = 45^0/135^0$ and uniaxial stress applied at $\varphi = 0^0/180^0$, (6) becomes

$$\Pi(45^0, 0^0) = \frac{\Pi_{11} + \Pi_{12}}{2} \tag{7}$$

The stress tensor $\boldsymbol{\sigma}$ is expressed as a function of its in-plane components

$$|\boldsymbol{\sigma}| = \sqrt{|\boldsymbol{\sigma_{11}}|^2 + |\boldsymbol{\sigma_{22}}|^2} \tag{8}$$

IV. Performance Comparison

The correctness and accuracy of the models are verified by comparing the Verilog-A description in Cadence© environment and FEM simulation results in COMSOL Multiphysics®. As shown in Table I, they are in excellent agreement, the difference between them being less than 0.15 %.

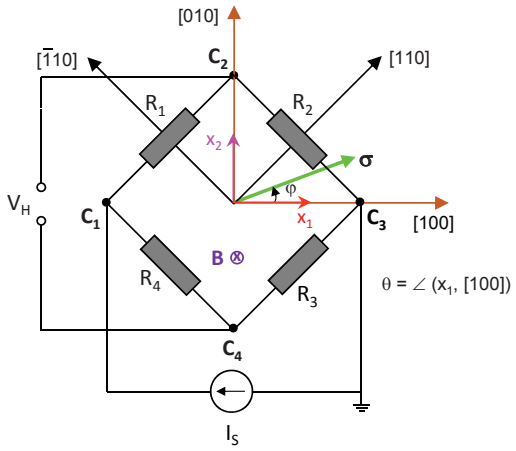

Fig. 5. Full Wheatstone-bridge circuit models the cross-shaped horizontal Hall-effect sensor. (x_1, x_2) is the in-plane cartesian coordinate system attached to the bridge. $([100], [010])$ are the principal Si-crystallographic axes in (001) Si-wafer plane. θ defines the bridge's position with respect to $[100]$-direction and φ the uniaxial stress application direction.

TABLE I
COMPARISON BETWEEN SIMULATION RESULTS OBTAINED WITH COMSOL MULTIPHYSICS® AND VERILOG-A

Magnetic / Stress		**COMSOL**		**VERILOG-A**	
$\lvert B\rvert$[mT]	$\lvert\sigma_{11}\rvert$[MPa]	V_H[mV]	S_I[V/AT]	V_H[mV]	S_I[V/AT]
0	0	0	0	0	0
0	250	0.00021	0.002	0.00209	0.002
100	0	7.1580	71.58	7.1436	71.436
100	250	7.1578	71.57	7.1434	71.434

V. CONCLUSION

This paper presents the simulation results of the bending-induced uniaxial stress effects on the performance of the ultra-thin magnetic sensors, for a standard 350 nm CMOS technology. The simulation results focus on magnetic sensor's sensitivity variation and offset drift induced by bending of the substrate. The results are the first step towards developing an on-chip compensation circuit for the piezoresistive effect that would allow accurate detection of the magnetic field in robotic and biomedical applications. The simulation results of the Hall-effect sensor using the Verilog-A model for a standard 350 nm CMOS technology, and those obtained by FEM simulation are in agreement.

As for the future work, we will perform experimental investigations of ultra-thin magnetic sensors during static and dynamic bending, for different in-plane orientations of the sensor and stress application directions. Moreover, the model will be extended by including the capacitances between the P^+ layer and the N-well and between the N-well and p-sub, for AC investigations. The effects of biaxial and shear stress on the sensor's performance will be also considered.

ACKNOWLEDGMENT

The research leading to these results received funding from Engineering and Physical Sciences Council (EPSRC) through the Fellowship for Growth - Printable Tactile Skin (EP/M002527/1) and EPSRC First Grant - FLEXELDEMO (EP/M002519/1).

REFERENCES

[1] R. S. Dahiya, P. Mittendorfer, M. Valle, G. Cheng, and V. Lumelsky, "Directions towards effective utilization of tactile skin – a review," *IEEE Sensors Journal*, vol. 13, no. 11, pp. 4121 – 4138, 2013.

[2] R. Dahiya and M. Valle, *Robotic Tactile Sensing - Technologies and System*. Springer, 2013.

[3] R. S. Dahiya, *Epidermal Electronics: Flexible Electronics for Biomedical Application*. Cambridge University Press, 2015, pp. 245–255.

[4] R. Dahiya, "Electronic skin," in *AISEM*, 2015, pp. 1–4.

[5] F. Axisa, P. M. Schmitt, C. Gehin, G. Delhomme, E. McAdams, and A. Dittmar, "Flexible technologies and smart clothing for citizen medicine, home healthcare, and disease prevention," *IEEE Trans. Information Tech. in Biomedicine,*, vol. 9, no. 3, pp. 325–336, 2005.

[6] M. Melzer, J. I. Mönch, D. Makarov, Y. Zabila, G. S. Cañón B., D. Karnaushenko, S. Baunack, F. Bahr, C. Yan *et al.*, "Wearable magnetic field sensors for flexible electronics," *Adv. Mater.*, 2014.

[7] M. Melzer, M. Kaltenbrunner, D. Makarov, D. Karnaushenko, D. Karnaushenko, T. Sekitani, T. Someya, and O. Schmidt, "Imperceptible magnetoelectronics," *Nat. comm.*, vol. 6, 2015.

[8] S. Jeon, G. Jang, H. Choi, and S. Park, "Magnetic navigation system with gradient and uniform saddle coils for the wireless manipulation of micro-robots in human blood vessels," *IEEE Trans Magn*, vol. 46, pp. 1943–1946, 2010.

[9] R. Dahiya and S. Gennaro, "Bendable ultra-thin chips on flexible foils," *IEEE Sensors J.*, vol. 13, no. 10, pp. 4030–4037, 2013.

[10] R. Magnani, F. Tinfena, V. Kempe, and L. Fanucci, "Mechanical stress measurement electronics based on piezo-resistive and piezo-hall effects," in *Elec., Circ. and Sys., 2002. 9th International Conference on*, vol. 1. IEEE, 2002, pp. 363–366.

[11] H. Heidari, U. Gatti, E. Bonizzoni, and F. Maloberti, "Low-noise low-offset current-mode hall sensors," in *9th Conf. Ph. D. Res. Microelectr. and Electron.*, 2013, pp. 325–328.

[12] H. Heidari, E. Bonizzoni, U. Gatti, and F. Maloberti, "A current-mode CMOS integrated microsystem for current spinning magnetic hall sensors," in *Circ. and Sys. (ISCAS), 2014 Int. Symp. on*. IEEE, 2014, pp. 678–681.

[13] M. Paun, J. Sallese, and M. Kayal, "Hall effect sensors design, integration and behavior analysis," *J. Sensor and Actuator Networks*, vol. 2, no. 1, pp. 85–97, 2013.

[14] R. Serway and J. Jewett, *Physics for scientists and engineers with modern physics*. Cengage learning, 2013.

[15] W. N. Sharpe Jr and W. N. Sharpe, *Springer handbook of experimental solid mechanics*. Springer Science & Business Media, 2008.

[16] B. Hälg, "Piezo-hall coefficients of n-type silicon," *J. Appl. Phys.*, vol. 64, no. 1, pp. 276–282, 1988.

[17] C. S. Smith, "Piezoresistance effect in germanium and silicon," *Phys. Rev.*, vol. 94, no. 1, p. 42, 1954.

[18] Y. Xu and H. Pan, "An improved equivalent simulation model for cmos integrated hall plates," *Sensors*, vol. 11, no. 6, pp. 6284–6296, 2011.

[19] S. Middelhoek and S. Audet, "Microelectronics and signal processing: Silicon sensors," 1989.

[20] J. Gere and S. Timoshenko, "Mechanics of materials brooks," *Cole, Pacific Grove, CA*, pp. 815–39, 2001.

[21] J. Kim, D. Cho, and R. S. Muller, "Why is (111) silicon a better mechanical material for mems," *Proc. Transd.*, pp. 662–665, 2001.

[22] N. Wacker, H. Richter, T. Hoang, M. Schlze, E. Angelopoulos, M. Hassan, and J. Burghartz, "Stress analysis of ultra-thin silicon chip-on-foil electronic assembly under bending," *Semiconductor Sc. and Tech.*, vol. 29, no. 9, pp. 1–12, 2014.

[23] N. Wacker, H. Richter, M. Hassan, H. Rempp, and J. N. Burghartz, "Compact modeling of cmos transistors under variable uniaxial stress," *Solid-State Electronics*, vol. 57, no. 1, pp. 52–60, 2011.